B_{12} Models with Highly Distorted N_4 Equatorial Ligation and a Co−C−N Ring: Structural Assessment of the Steric Influence of Benzimidazole and Imidazole Axial Ligands

Luigi G. Marzilli,* Suzette M. Polson, Lory Hansen, Scott J. Moore, and Patricia A. Marzilli

Department of Chemistry, Emory University, Atlanta, Georgia 30322

Received January 8, 1997[⊗]

In human B_{12} enzymes, a histidyl imidazole is the lower axial ligand instead of the benzimidazole of the coenzymes. We have explored the differences in the binding interactions of these ligands using a novel class of organocobalt models, [LCo(*N*-CH_2-CHEL)]X, with an unusually spacious lower coordination site created by a rare Co−C−N ring. We now compare two new analogs, **1** (L = 1,5,6-trimethylbenzimidazole = Me_3Bzm) and **2** (L = *N*-methylimidazole = *N*-MeImd), with the first analog, **3** (L = pyridine = py). The three structures (X = PF_6 for **1** and **2**; X = ClO_4 for **3**) have similar geometrical parameters for the ring atoms (N(2), Co, C(12)). A pocket under the Co−C−N group is created by the raised position of N(2) above the plane of the other three equatorial N donors, the *cis* oxime N, N(1), the *trans* oxime N, N(4), and the *cis* imine N, N(3). A net upward bending is clearly shown by the sum of the four *cis* N−Co−N bond angles involving the L ligating atom, N(5). The sum is ∼23° more in the new models than in related imine/oxime-type (I/O) models. The distortions around N(5) differ significantly for the three structures. The Co−N(5) bond of Me_3Bzm complex **1** is tilted furthest away from the Co−C−N pocket, and the N(5)−Co−N(2) angle is 111°. The value of the N(5)−Co−N(4) angle (96°) is close to that of the related angle (95°) in the I/O model, [Me_3BzmCo((DO)(DOH)pn)CH_3]PF_6. In contrast, the N(5)−Co−N(4) angle of the *N*-MeImd and the py complexes, **2** and **3**, is larger than that in I/O complexes, suggesting that these L ligands are small enough to move toward the pocket. These and other structural parameters suggest clear differences between the steric interactions of the equatorial ligand with the imidazole and with the benzimidazole ligands. These complexes have unusual ^{1}H NMR properties, e.g. a large remote isotope effect on some CH signals after exchange of the oxime OH to OD. At pH 13, the N_4C chelate of [H_2OCo(*N*-CH_2-CHEL)]$^+$ reverts, in part, to the classical I/O N_4 chelate, suggesting a stepwise mechanism involving C−N bond cleavage to form a Co−CH_2OH intermediate, which then undergoes base-catalyzed Co−C bond cleavage.

Introduction

We recently discovered a new class of synthetic organocobalt B_{12} models formed by a novel synthetic route. Base transforms the imine/oxime (I/O) B_{12} model complexes [LCo((DO)(DOH)pn)CH_2Br]$^+$ (upper left, Chart 1, R = CH_2Br) into [LCo(*N*-CH_2-CHEL)]$^+$ complexes (*N*-CH_2-CHEL = new N_4C chelate shown at the upper left of Chart 2).[1] These unusual [LCo(*N*-CH_2-CHEL)]$^+$ species contain a Co−C bond considerably distorted from the normal orientation (the Co−C bond direction is tilted ∼26° away from that normally found); the distortion is referred to as *θ*-bending (Chart 3).[1] Studies of the *N*-CH_2-CHEL complexes provided evidence that Co−C *θ*-bending was not a favorable pathway for Co−C bond weakening and cleavage by B_{12}-dependent enzymes,[1] in support of MO calculations.[2]

Our primary interest in these new models was in elucidating the facility of C−N bond formation and the influence of *θ*-bending. In our study of the pyridine complex [pyCo(*N*-CH_2-CHEL)]ClO_4,[1] we noted that the Co−C−N ring distorts the coordination geometry, creating a pocket under the Co−N(2) bond on the L face of the macrocycle. The ring nitrogen, N(2), is raised ∼0.7 Å above the normally coplanar four-nitrogen plane. This distortion in the equatorial macrocycle in [pyCo(*N*-CH_2-CHEL)]ClO_4 affords an opportunity to investigate steric influences. An important feature of the corrin rings of B_{12} compounds, and one not normally present in models, is the extensive puckering of the equatorial ligand. The recent discovery of the replacement of the coordinated 5,6-dimethylbenzimidazole ring in cobalamin coenzymes when these bind to methionine synthase[3] and to methylmalonyl-CoA mutase[4] has spurred renewed interest in the steric and electronic *trans* influence of L ligands in B_{12} compounds. The comparison of imidazole and benzimidazole compounds is particularly relevant

Chart 1. B_{12} Model Complexes

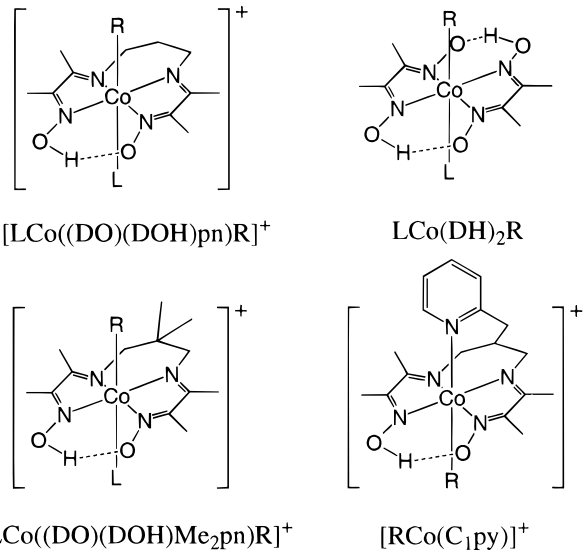

⊗ Abstract published in *Advance ACS Abstracts,* August 1, 1997.

(1) Polson, S. M.; Hansen, L.; Marzilli, L. G. *J. Am. Chem. Soc.* **1996**, *118*, 4804.
(2) Zhu, L.; Kostic, N. M. *Inorg. Chem.* **1987**, *26*, 4194.
(3) Drennan, C. L.; Huang, S.; Drummond, J. T.; Matthews, R. G.; Ludwig, M. L. *Science* **1994**, *266*, 1669.
(4) Mancia, F.; Keep, N. H.; Nakagawa, A.; Leadlay, P. F.; McSweeney, S.; Rasmussen, B.; Bosecke, P.; Diat, O.; Evans, P. R. *Structure* **1996**, *4*, 339.

S0020-1669(97)00022-0 CCC: $14.00

Chart 2. Complexes Containing the Co−C−N Ring

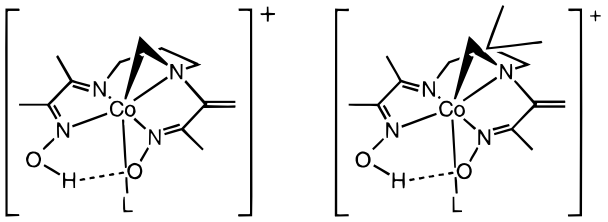

$[LCo(N\text{-}CH_2\text{-}CHEL)]^+$ $[LCo(N\text{-}CH_2\text{-}Me_2pnCHEL)]^+$

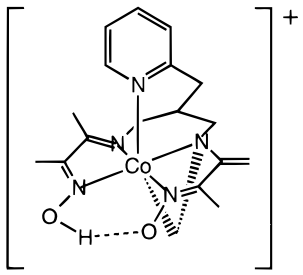

$[Co(N\text{-}CH_2\text{-}C_1pyCHEL)]^+$

Chart 3. θ-Bending of the Co−C Bond

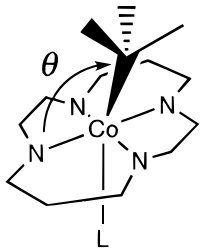

since the group substituting for 5,6-dimethylbenzimidazole is an imidazole from a protein side chain.[3,4] We hypothesized that steric bias for one side of the macrocycle would be manifest in the orientation of the sterically lopsided axial benzimidazole and that the bulky part of such a ligand would lie under the pocket created by the Co−C−N ring. For these reasons, *N*-CH_2-CHEL complexes containing Me_3Bzm and *N*-MeImd were prepared and characterized crystallographically.

During the course of examining the structural features of these products, we discovered some unusual NMR behavior, which we describe here. As an aid in interpreting these data, we examined two related I/O B_{12} models ((DO)(DOH)Me_2pn and C_1py, Chart 1) and compared our results to those for a standard model system, the cobaloximes (upper right, Chart 1). Our original study of the formation of the Co−C−N ring was impeded by product instability at high pH.[1] We have now found that high pH leads to reversion of the N_4C chelate to the traditional N_4 chelate and that this process is accompanied by Co−C bond cleavage.

Experimental Section

Synthesis. Co((DO)(DOH)pn)Br_2,[5,6] $[H_2OCo(N\text{-}CH_2\text{-}CHEL)]ClO_4$,[1] $[H_2OCo((DO)(DOH)pn)CH_2Br]ClO_4$,[7] Co((DO)(DOH)$Me_2$pn)$Br_2$,[8] $[BrCo(C_1py]ClO_4$,[9] and Me_3Bzm[10] were prepared as previously reported. $[N$-MeImdCo((DO)(DO)pn)$CH_2Br]PF_6$ was made by the procedure for the ClO_4 salt,[7] substituting KPF_6 for $NaClO_4$. The preparation of $(CO)Co^I$((DO)(DOH)Me_2pn) was similar to the method used for $(CO)Co^I$((DO)(DOH)pn).[11] *Caution! Perchlorate salts may be explosive and should be handled in small quantities with appropriate precautions.*[12] ^{1}H NMR spectra were recorded on GE QE-300 and GE GN-600 Omega NMR instruments. Elemental analyses were performed by Atlantic Microlabs, Atlanta, GA.

$[Me_3BzmCo(N\text{-}CH_2\text{-}CHEL)]ClO_4$. A solution of $[H_2OCo(N\text{-}CH_2\text{-}CHEL)]ClO_4$ (0.15 g, 0.35 mmol) in MeOH (10 mL) and acetone (3 mL) was treated with Me_3Bzm (0.062 g, 0.38 mmol, in 1 mL of MeOH). The resulting solution was stirred overnight at room temperature, and a fine yellow solid precipitated; this solid was collected on a frit, washed with ether, and vacuum-dried. Yield: 0.12 g (55%). $[Me_3BzmCo(N\text{-}CH_2\text{-}CHEL)]PF_6\cdot CH_2Cl_2$ (**1**) was prepared by treating an acetone/H_2O (1:1) solution of the perchlorate salt with aqueous KPF_6, precipitating an orange solid. The solid was recrystallized as orange prisms from CH_2Cl_2.

$[N$-MeImdCo(N-CH_2-CHEL)]PF_6 (2). This compound was prepared according to the procedure used for the perchlorate salt,[1] using $[N$-MeImdCo((DO)(DO)pn)$CH_2Br]PF_6$. Yield: 48%. The solid was recrystallized from acetone/H_2O as red-orange prisms.

$[(N\text{-MeImd})_2Co((DO)(DOH)pn)](ClO_4)_2$. A suspension of Co((DO)(DOH)pn)Br_2 (0.75 g, 1.6 mmol) in a 1:1 MeOH/H_2O solution (75 mL) was treated with *N*-MeImd (0.29 mL, 3.6 mmol). $AgNO_3$ (0.56 g, 3.3 mmol) was then added to the red solution. After the mixture was stirred for 30 min, AgBr was removed by filtration. An aqueous solution of $NaClO_4\cdot H_2O$ (1.0 g, 7.2 mmol) was added to the red solution. The solvent was removed by rotary evaporation, and acetone was added to the residue. Undissolved material was removed by filtration, and the solvent was removed from the red filtrate by rotary evaporation. The solid remaining was collected, washed thoroughly with H_2O, and vacuum-dried. Yield: 0.56 g (52%).

$[H_2OCo((DO)(DOH)Me_2pn)CH_2Br]PF_6$. Under nitrogen, a blue-green solution of $(CO)Co^I$((DO)(DOH)Me_2pn) (0.30 g, 0.85 mmol) in THF (53 mL) was treated with CH_2Br_2 (0.59 mL, 8.5 mmol). Overnight, the stirred solution turned red, and the THF was then removed by rotary evaporation. A solution of the resulting red air-stable solid in a 1:1 MeOH/acetone solution (40 mL) was filtered to remove undissolved impurities. After the volume was reduced by ~50%, the solution was diluted with H_2O (20 mL) and treated with $AgNO_3$ (0.067 g, 0.40 mmol). After the mixture was stirred for 30 min, AgBr was removed by filtration through Celite. Addition of a solution of KPF_6 (1.1 g in H_2O) induced immediate precipitation. The mixture was chilled overnight, and the orange powder was then collected, washed with cold H_2O, and dried under vacuum. Yield: 0.14 g (28%).

$[N$-MeImdCo(N-CH_2-Me_2pnCHEL)]PF_6. Crude $[N$-MeImdCo((DO)(DOH)Me_2pn)$CH_2Br]PF_6$ was prepared by treating a stirred suspension of $[H_2OCo((DO)(DOH)Me_2pn)CH_2Br]PF_6$ (0.14 g, 0.24 mmol) in CH_2Cl_2 (15 mL) with *N*-MeImd (0.058 mL, 0.72 mmol). The next day, the mixture was filtered and CH_2Cl_2 was removed from the filtrate by rotary evaporation to give a red oil. Water was added to a solution of the oil in MeOH until it became cloudy. From the mixture, chilled overnight, was collected an orange precipitate (0.11 g), which was washed with H_2O and dried under vacuum. Most of the material (0.10 g, 0.16 mmol) was added under nitrogen to a degassed solution of Na (0.018 g, 0.8 mmol) in degassed MeOH (23 mL); the mixture was stirred overnight and then filtered through a fine frit, and most of the MeOH was removed by rotary evaporation. H_2O was added to the red solution, and an orange solid precipitated. The solution was kept in a refrigerator overnight, and the solid was collected, washed with cold H_2O and Et_2O, and vacuum-dried. Yield: 0.032 g (36%).

$[BrCH_2Co(C_1py)]ClO_4$. A suspension of $[BrCo(C_1py]ClO_4$ (0.50 g, 0.88 mmol) in MeOH (75 mL) was treated with a solution of NaOH (0.075 g, 1.9 mmol in 2 mL of H_2O). The red solution was purged with nitrogen for 10 min before CH_2Br_2 (0.18 mL, 2.6 mmol) was added. An aqueous solution of $NaBH_4$ (0.050 g, 1.3 mmol, in 8 mL)

(5) Parker, W. O., Jr. Ph.D. Thesis, Emory University, 1987.
(6) Costa, G.; Mestroni, G.; de Savorgnani, E. *Inorg. Chim. Acta* **1969**, *3*, 323.
(7) Parker, W. O., Jr.; Zangrando, E.; Bresciani-Pahor, N.; Marzilli, P. A.; Randaccio, L.; Marzilli, L. G. *Inorg. Chem.* **1988**, *27*, 2170.
(8) Yohannes, P. G.; Bresciani-Pahor, N.; Randaccio, L.; Zangrando, E.; Marzilli, L. G. *Inorg. Chem.* **1988**, *27*, 4738.
(9) Gerli, A.; Sabat, M.; Marzilli, L. G. *J. Am. Chem. Soc.* **1992**, *114*, 6711.
(10) Charland, J.-P.; Zangrando, E.; Bresciani-Pahor, N.; Randaccio, L.; Marzilli, L. G. *Inorg. Chem.* **1993**, *32*, 4256.
(11) Polson, S. M.; Cini, R.; Pifferi, C.; Marzilli, L. G. *Inorg. Chem.* **1997**, *36*, 314.
(12) Raymond, K. N. *Chem. Eng. News* **1983**, *61* (Dec 5), 4.

Table 1. Crystallographic Data for **1** and **2**

	1	**2**
empirical formula	$C_{22}H_{32}CoF_6N_6O_2P{\cdot}CH_2Cl_2$	$C_{16}H_{26}CoF_6N_6O_2P$
fw	701.36	538.3
space group	$P2_1/c$	$P2_1/c$
a, Å	12.424(3)	10.340(2)
b, Å	14.353(7)	13.915(3)
c, Å	17.412(11)	15.433(3)
β, deg	108.88(3)	96.85(3)
V, Å^3	2938(2)	2204.6(11)
Z	4	4
D(calc), mg/m^3	1.586	1.622
abs coeff, mm^{-1}	0.892	0.927
radiation (λ, = Å)	MoKα (0.710 73)	MoKα (0.710 73)
temp, K	173	173
min/max transm	0.36/0.44	0.36/0.40
final *R* indices, %	$R = 7.45$, w$R2 = 15.18$[a]	$R = 4.73$, Rw $= 6.90$[b]
R indices (all data), %	$R = 8.05$, w$R2 = 15.43$	$R = 5.42$, Rw $= 7.08$

[a] $I > 2\sigma(I)$; w*R*2 refined on F^2. [b] $I > 4\sigma(I)$.

was then added dropwise with stirring. After 15 min, acetone (10 mL) was added and the N_2 flow was stopped. The solution was diluted with H_2O (60 mL), treated with $AgNO_3$ (0.52 g), and stirred for 30 min. The silver salts were removed by filtration through Celite. The volume was reduced to 50 mL by rotary evaporation, and the solution was chilled (~5 °C). The yellow precipitate that formed overnight was collected and washed with cold H_2O and Et_2O. Yield: 0.10 g (20%).

[Co(*N*-CH$_2$-C$_1$pyCHEL)]ClO$_4$. Under a nitrogen atmosphere, Na (0.060 g, 2.6 mmol) was dissolved in degassed MeOH (10 mL) in a Schlenk flask. A degassed MeOH solution of [BrCH$_2$Co(C$_1$py)]ClO$_4$ (0.30 g, 0.51 mmol in 25 mL) was introduced by cannula. The solution was stirred overnight under nitrogen, and MeOH was removed by rotary evaporation. A CH_2Cl_2 solution of the resulting dark red oil was filtered and extracted with H_2O three times, and the combined aqueous extracts were back-extracted with CH_2Cl_2. The combined organic phase was dried over $MgSO_4$. The orange-yellow solid obtained after CH_2Cl_2 removal was dissolved in acetone and the solution filtered through a cotton-plugged pipet. Solvent was removed by rotary evaporation, and the residue was redissolved in 4:1 MeOH/H_2O and placed in the refrigerator. The orange solid that formed after several days was collected and washed with Et_2O.

Solution Studies at pH 13. An aliquot (0.58 mL) of a stock solution of [H$_2$OCo((DO)(DOH)pn)CH$_2$Br]ClO$_4$ (0.0112 g in 8 mL of H_2O) was added to a pH 13 (NaOH) solution (2.30 mL). The reaction was quenched at various times by neutralizing with HNO_3 to pH 7. H_2O was removed by rotary evaporation. A slight excess of *N*-MeImd (2.2 equiv) was added to a MeOH solution of the residue, and the solvent was removed. Inorganic salts were removed by extracting the residue with CH_2Cl_2 and filtering. The solid isolated upon removal of CH_2Cl_2 was washed with Et_2O. ^{1}H NMR spectra were recorded in DMSO-d_6.

Isolation of 4 (Cf. Results and Discussion). [H$_2$OCo((DO)(DOH)-pn)CH$_2$Br]ClO$_4$ (0.090 g, 0.18 mmol) was added to freshly made pH 13 NaOH (400 mL). After 50 min, the reaction was quenched with 3 M HNO_3. *N*-MeImd (0.022 mL) was added, and the solvent was removed. The residue was repeatedly extracted with $CHCl_3$. The $CHCl_3$-insoluble residue was extracted with MeOH to give primarily **4**. When the $CHCl_3$ fraction showed (by ^{1}H NMR spectroscopy) the presence of a significant amount of **4**, the trituration procedure was repeated using a smaller volume of $CHCl_3$. The 0.006 g of **4** that was isolated by this procedure was treated with an aqueous solution of KPF_6, and the precipitate that formed was collected and washed with H_2O.

X-ray Crystallography. An orange crystal of [Me$_3$BzmCo(*N*-CH$_2$-CHEL)]PF$_6$·CH$_2$Cl$_2$ (**1**) (0.60 × 0.46 × 0.39 mm, recrystallized from CH_2Cl_2) and a red-orange crystal of [*N*-MeImdCo(*N*-CH$_2$-CHEL)]PF$_6$ (**2**) (0.40 × 0.40 × 0.50 mm, from acetone/H_2O) were used for data collection. Intensity data were collected on a Siemens P4 instrument at −100 °C using an LT2 low-temperature device and corrected for Lorentz and monochromator polarization, extinction (**1** only), and absorption (semiempirical method based on azimuthal scans). Crystal data and refinement parameters are presented in Table 1.

The structure of **1** was solved by Patterson methods and refined by full-matrix least-squares procedures on F^2 using SHELXL-93. The central carbon of the 1,3-propanediyl bridge, C(6), was disordered and refined in two positions, one above (C(6a), 70% occupancy) and the other below (C(6b), 30% occupancy) the N_4 basal coordination plane. F(6) was also disordered and refined in three positions with 50% (F(6a)), 20% (F(6b)), and 30% (F(6c)) occupancies. All non-hydrogen atoms were refined anisotropically. H atoms were generated at calculated positions (d(C−H) = 0.96 Å, d(O−H) = 0.84 Å) and constrained using a riding model with isotropic thermal parameters that were 20% greater than the U(eq) of the heavy bonded atom. The oxime H atom was assigned to O(2).

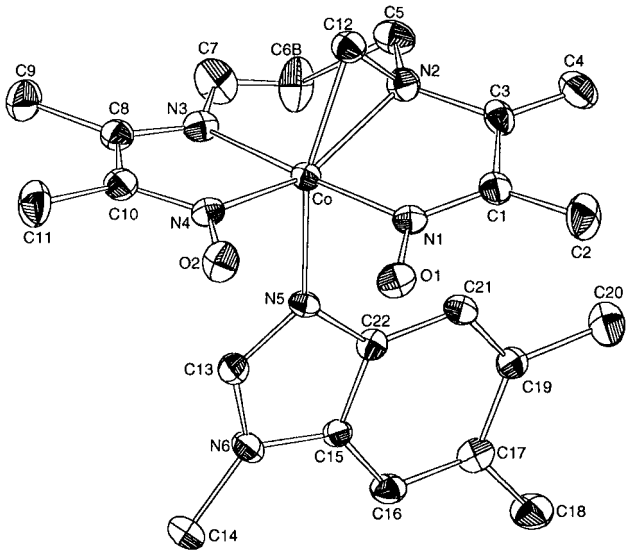

Figure 1. Perspective drawing of **1** with 30% probability for the thermal ellipsoids.

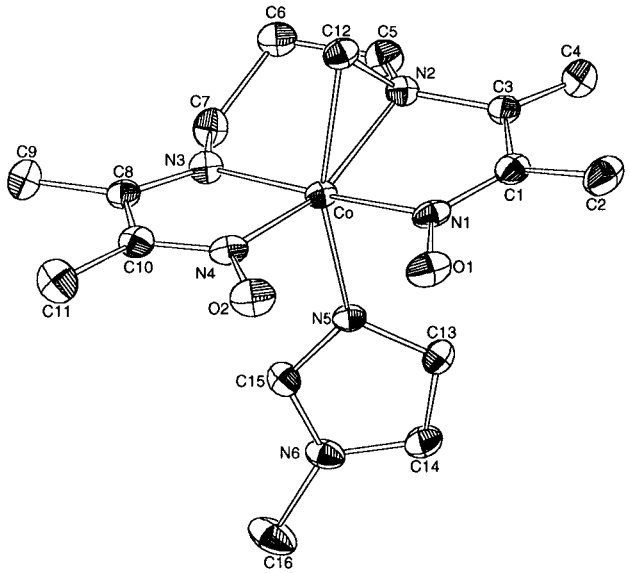

Figure 2. Perspective drawing of **2** with 30% probability for the thermal ellipsoids.

The structure of [*N*-MeImdCo(*N*-CH$_2$-CHEL)]PF$_6$ (**2**) was solved by direct methods, and all non-hydrogen atoms were refined by full-matrix least-squares procedures using SHELXTL PLUS (VMS). Two oxime H atoms, each with half-occupancy, were observed in the difference map and included in the refinement. The C(6) and C(12) H atoms were also located from difference maps. All other H atoms were generated at calculated positions (d(C−H) = 0.96 Å). All H atoms were constrained using a riding model with isotropic thermal parameters fixed at 0.05.

Results and Discussion

X-ray Structural Studies. The Co−C−N rings of [Me$_3$-BzmCo(*N*-CH$_2$-CHEL)]PF$_6$·CH$_2$Cl$_2$ (**1**) and [*N*-MeImdCo(*N*-CH$_2$-CHEL)]PF$_6$ (**2**) (Figures 1 and 2) and the previously reported [pyCo(*N*-CH$_2$-CHEL)]ClO$_4$ (**3**)[1] are similar (Table 2).

Table 2. Selected Bond Lengths (Å) and Bond Angles (deg) for Complexes of the Type $[LCo(N\text{-}CH_2\text{-}CHEL)]^+$ (L = Me_3Bzm (**1**), *N*-MeImd (**2**), py (**3**))

	Me_3Bzm	*N*-MeImd	py[a]
	Bond Lengths		
Co−C	1.913(7)	1.932(5)	1.927(5)
Co−N(1)	1.899(5)	1.900(4)	1.886(5)
Co−N(2)	1.968(5)	1.938(4)	1.943(5)
Co−N(3)	1.897(5)	1.897(4)	1.895(5)
Co−N(4)	1.874(5)	1.879(4)	1.878(6)
C(12)−N(2)	1.443(8)	1.441(6)	1.445(8)
Co−N(5)	2.052(5)	2.036(4)	2.068(5)
	Bond Angles		
N(2)−Co−C(12)	43.6(3)	43.7(2)	43.8(2)
Co−N(5)−C	124.5(4)[b]	125.9(3)[b]	121.5(4)
	131.2(4)	129.0(3)	121.2(5)
N(1)−Co−N(5)	92.4(2)	93.5(2)	92.6(2)
N(2)−Co−N(5)	111.4(2)	104.8(1)	107.1(2)
N(3)−Co−N(5)	91.3(2)	91.4(1)	91.7(2)
N(4)−Co−N(5)	96.1(2)	98.5(1)	99.6(2)
C(12)−Co−N(5)	155.0(2)	148.4(2)	150.9(2)

[a] Reference 1. [b] Angle containing the C atom next to N(6) [Co−N(5)−C(13) for **1**; Co−N(5)−C(15) for **2**].

The Co−N(2) bond length in the Co−C−N ring increases across the series *N*-MeImd < py < Me_3Bzm, with a significant difference between those for **1** and **2**. However, the N(2)−Co−C(12) bond angle is essentially the same for **1**, **2**, and **3**, ∼44° (Table 2). The Co−C bond length decreases in the order *N*-MeImd > py > Me_3Bzm, but the differences are not significant. Thus, although these are highly distorted species, they fit in with other organometallic complexes with macrocyclic nitrogen or oxygen donor ligands.[13] In all such complexes, the Co−C bond length has been found to vary little for a given R when L is an N-donor.[13,14] Only when the *trans* ligand is a strong donor (e.g., an alkyl or a phosphine) does the Co−C bond lengthen slightly.[13−15]

The Co−N(5) bond length of the $[LCo(N\text{-}CH_2\text{-}CHEL)]^+$ complexes increases slightly in the order *N*-MeImd < Me_3Bzm < py, with a barely significant difference between **2** (L = *N*-MeImd) and **3** (py). The similar bond lengths contrast with previous findings; in cobaloximes and I/O type complexes, the bond lengths for Me_3Bzm and py were similar but significantly longer than that for *N*-MeImd.[7] These earlier findings led to the conclusion that the effective bulk of Me_3Bzm is not significantly different from that of py.[7] However, for $[LCo(N\text{-}CH_2\text{-}CHEL)]^+$ complexes, the bulk of L does not appear to be so important in influencing bond length. The angles about the Co−N(5) bond (see below) do seem to be sensitive to the shape and the effective bulk of L.

Some geometrical parameters of **1** and **2** are comparable to those of I/O type models, $[LCo((DO)(DOH)pn)R]PF_6$. The Co−N(5) bond length and Co−N(5)−C bond angles of **2** are similar to those of $[N\text{-MeImdCo}((DO)(DOH)pn)CH_3]PF_6$[16] (Table 3). Thus, the CH_2 group of the Co−C−N ring has a *trans* influence like that for the compound with R = CH_3, a moderate alkyl donor. In addition, the two Co−N(5)−C bond angles for **1** are similar to some of those found in structures of $[Me_3BzmCo((DO)(DOH)pn)R]PF_6$ complexes (Table 4).

The total of the four *cis* N−Co−N bond angles involving the axial N(5) may be the best indicator of the overall bulk of L in these distorted $[LCo(N\text{-}CH_2\text{-}CHEL)]^+$ complexes and in the I/O models. For the more widely studied I/O complexes, there is a definite correlation between ligand bulk and the sum of the *cis* N−Co−(L ligating atom) angles (Supporting Information). In I/O complexes of the type $[LCo((DO)(DOH)pn)CH_3]^+$, these angles total 370° for L = Me_3Bzm,[7] ∼369° for L = P-donor,[17] 368° for L = py,[18] 366° for L = *N*-MeImd,[16] 360° for L = aniline,[19] and ∼355° for L = H_2O.[5,20] The structures for $[LCo(N\text{-}CH_2\text{-}CHEL)]^+$ complexes exhibit angles totaling 391° for both the L = Me_3Bzm and L = py complexes and 388° for the L = *N*-MeImd complex. Differences in the planar N-donor ligands appear to cause similar differences in the total angle, thus affecting the equatorial ligand similarly for both series of complexes. The larger total (∼23°) in the new models than in related I/O models clearly shows a greater net inherent upward bending of the four equatorial N's of the $N\text{-}CH_2$-CHEL chelate (Supporting Information).

While the sum of all the N−Co−N(5) angles provides useful information about overall ligand bulk, one angle in particular (N(4)−Co−N(5), which is directly opposite to the distorted portion of the macrocycle for $[LCo(N\text{-}CH_2\text{-}CHEL)]^+$ complexes) appears to be sensitive to L shape. The value of this angle is 96° for **1**, close to that of a related angle (95°) in the

Table 3. Selected Bond Lengths (Å) and Bond Angles (deg) for Complexes of the Type $[LCo((DO)(DOH)pn)CH_3]PF_6$ (L = Me_3Bzm, *N*-MeImd, py)[a]

	Me_3Bzm[b]	*N*-MeImd[c]	py[d]
	Bond Lengths		
Co−C	2.011(3)	2.001(3)	2.003(3)
Co−N(2)	1.909(3)	1.914(2)	1.918(3)
Co−N(5)	2.100(3)	2.042(2)	2.106(3)
	Bond Angles		
N(2)−Co−C	87.6(1)	87.5(1)	87.2(1)
Co−N(5)−C	122.8(2)	125.7(2)	121.2(5)
	132.2(2)	129.1(2)	121.5(4)
N(1)−Co−N(5)	94.8(1)	92.3(1)	93.7(1)
N(2)−Co−N(5)	95.0(1)	90.55(9)	91.1(1)
N(3)−Co−N(5)	91.6(1)	90.07(9)	91.3(1)
N(4)−Co−N(5)	89.0(1)	93.51(9)	91.8(1)
C−Co−N(5)	177.4(1)	179.2(1)	178.9(1)

[a] Atoms N(2) and N(4) were reassigned to reflect the same order of N atoms as in this work. [b] Reference 7. [c] Reference 16. [d] Reference 18.

Table 4. Geometrical Data for **1** and for the Relevant $[Me_3BzmCo((DO)(DOH)pn)R]PF_6$ Complexes

R	Co−C, Å	Co−N(5), Å	Co−N(5)−C, deg
		N-CH_2-CHEL	
N-CH_2	1.913(7)	2.052(5)	124.5(4)
			131.2(4)
		(DO)(DOH)pn	
CH_2CF_3[a]	2.026(4)	2.060(3)	123.1(2)
			132.4(2)
CH_2Cl[b]	2.020(4)	2.088(3)	121.8(3)
			133.3(3)
CH_3[a]	2.011(3)	2.100(3)	122.8(2)
			132.3(2)
CH_2CH_3[a]	2.041(3)	2.105(3)	122.4(3)
			133.1(2)
CH_2OCH_3[b]	2.065(5)	2.133(4)	121.7(4)
			132.3(4)

[a] From reference 7. [b] From reference 11.

(13) Randaccio, L.; Bresciani-Pahor, N.; Zangrando, E.; Marzilli, L. G. *Chem. Soc. Rev.* **1989**, *18*, 225.
(14) Bresciani-Pahor, N.; Forcolin, M.; Marzilli, L. G.; Randaccio, L.; Summers, M. F.; Toscano, P. J. *Coord. Chem. Rev.* **1985**, *63*, 1.
(15) Calligaris, M. *J. Chem. Soc., Dalton Trans.* **1974**, 1628.
(16) Bresciani-Pahor, N.; Randaccio, L.; Zangrando, E. *Inorg. Chim. Acta* **1990**, *168*, 115.
(17) Parker, W. O., Jr.; Bresciani-Pahor, N.; Zangrando, E.; Randaccio, L.; Marzilli, L. G. *Inorg. Chem.* **1986**, *25*, 1303.
(18) Parker, W. O., Jr.; Bresciani-Pahor, N.; Zangrando, E.; Randaccio, L.; Marzilli, L. G. *Inorg. Chem.* **1985**, *24*, 3908.
(19) Parker, W. O., Jr.; Zangrando, E.; Bresciani-Pahor, N.; Randaccio, L.; Marzilli, L. G. *Inorg. Chem.* **1986**, *25*, 3489.
(20) Brückner, S.; Calligaris, M.; Nardin, G.; Randaccio, L. *Inorg. Chim. Acta* **1969**, *3*, 278.

Table 5. ^{1}H NMR Shifts (ppm) of Me_3Bzm, $[Me_3BzmCo(N\text{-}CH_2\text{-}CHEL)]ClO_4$, and $[Me_3BzmCo(chelate)CH_3]^{(+/0)}$(or ClO_4) Complexes in $CDCl_3$

chelate	H2	H4	H7	B11H3	B10H3	OH···O	C═CH_2	NCH_2CCH_2N		imine CH_3	oxime CH_3	NCH_3	$CoCH_2$
$N\text{-}CH_{2-CHEL}$[a]	7.99	7.22	7.15	2.36	2.31	18.79	5.38	2.96	4.12	2.19	1.99	3.96	3.10
							5.85	3.56			2.43		3.95
$(DH)_2$[b]	7.95	7.98	7.08	2.37	2.35	18.62					2.10	3.74	
(DO)(DOH)pn[c]	7.66	7.26	7.15	2.34	2.32	19.22		3.79	4.10	2.41	2.29	3.91	
$(DO)(DOH)Me_{2pn}$[d]	7.37	6.69	7.14	2.32	2.26	18.72		3.54		2.54	2.39	3.88	
Me_{3Bzm}[b]	7.74	7.55	7.15	2.40	2.38							3.78	

[a] Acetone signal at 2.17 ppm. [b] Reference 7. [c] Reference 11. [d] Reference 24.

Table 6. ^{1}H NMR Shifts (ppm) of *N*-MeImd, $[N\text{-}MeImdCo(N\text{-}CH_2\text{-}CHEL)]ClO_4$, and $[N\text{-}MeImdCo(chelate)CH_3]^{(+/0)}$(or ClO_4) Complexes in $CDCl_3$

chelate	H2	H4	H5	OH···O	C═CH_2	NCH_2CCH_2N		imine CH_3	oxime CH_3	NCH_3	$CoCH_2$
$N\text{-}CH_2\text{-}CHEL$[a]	7.75	6.64	6.97	18.87	5.29	3.13	3.65	2.28	2.04	3.84	3.00
					5.67	3.45	3.82		2.36		3.91
$(DH)_2$[b]	7.44	6.96	6.78	18.38					2.14	3.64	
(DO)(DOH)pn[b]	7.54	6.43	6.83	18.90		3.68	4.04	2.42	2.30	3.78	
N-MeImd[b]	7.41	7.03	6.87							3.68	

[a] 600 MHz data. [b] Reference 19.

Table 7. ^{1}H NMR Shifts (ppm) of py, $[pyCo(N\text{-}CH_2\text{-}CHEL)]ClO_4$, and $[pyCo(chelate)CH_3]^{(+/0)}$(or ClO_4) Complexes in $CDCl_3$

chelate	α	β	γ	C═CH_2	OH···O	NCH_2CCH_2N		imine CH_3	oxime CH_3	$CoCH_2$
$N\text{-}CH_2\text{-}CHEL$	8.25	7.60	7.92	5.41	18.62	2.93	3.89	2.28	2.04	3.15
				5.83		3.54	3.97		2.41	4.09
$(DH)_2$[a]	8.61	7.33	7.73		18.32				2.13	
(DO)(DOH)pn[a]	8.03	7.56	7.80		18.80	3.79	4.07	2.45	2.30	
$N\text{-}CH_2\text{-}C_1py\text{-}CHEL$	8.58	7.31	7.77	5.26	19.09	3.40	4.36	2.11	1.99	3.42
		7.46		5.76		3.73		2.26		4.04
C_{1py}[b]	8.31	7.14	7.65		19.30	3.93	4.36	2.37	2.23	
		7.40								
py[a]	8.61	7.29	7.68							

[a] Reference 7. [b] Reference 23.

I/O model $[Me_3BzmCo((DO)(DOH)pn)CH_3]PF_6$.[7] In contrast, the N(4)−Co−N(5) angles in the *N*-MeImd and py complexes, **2** and **3**, are larger than those in I/O complexes (Tables 2 and 3), suggesting that these L ligands are small enough to move toward the pocket created by the three-membered ring. Indeed, for $[LCo(N\text{-}CH_2\text{-}CHEL)]^+$, the *N*-MeImd (**2**) and py (**3**) complexes have smaller N(2)−Co−N(5) angles than the Me_3-Bzm complex (**1**).

The orientation of the L plane can be described by the torsion angle ϕ [N*−Co−N(5)−C*, where N* is the midpoint between the oxime nitrogens, N(1) and N(4); C* is either the C next to N(5) with an acute ϕ for C_2-symmetrical L or the C on the less bulky L side for lopsided L]. For the I/O complexes $[Me_3$-$BzmCo((DO)(DOH)pn)R]PF_6$, ϕ falls into two ranges, ∼55−80 and ∼115−120°, with the bulky six-membered ring under the imine half and the oxime half, respectively.[7,11] The value for ϕ in **1** (66°) places it in the first range, consistent with the distorted side of the macrocycle having a smaller steric influence. However, the bulk of the Me_3Bzm ligand in **1** is oriented ∼20° away from the deepest part of the cavity (along the Co−N(2) bond). This finding may explain the larger N(2)−Co−N(5) angle in **1** than in **2** or **3** (Table 2); this reasoning is valid even if packing forces influence ϕ.

^{1}H NMR Spectroscopy. The ^{1}H NMR spectra of $[LCo(N\text{-}CH_2\text{-}CHEL)]^+$ complexes have unique features (Tables 5−7), including a 1 ppm dispersion of the signals of the geminal $N\text{-}CH_2$ protons.[1] Normally, the coupling constant is large for geminal protons on sp^3-hybridized carbons. However, the $N\text{-}CH_2$ protons are not coupled, suggesting that the $N\text{-}CH_2$ carbon has considerable sp^2 character.[21] In the upfield region, the equatorial imine CH_3 group signal for $[N\text{-}MeImdCo(N\text{-}CH_2\text{-}CHEL)]ClO_4$ in $CDCl_3$ was a doublet (2.28 ppm, ∼1 Hz) instead of the expected singlet. 2-D NMR techniques (ROESY) were used to determine the proton to which the methyl group was coupled. The methyl group protons exhibited coupling to a proton on the first carbon of the 1,3-propanediyl bridge, a five-bond homoallylic coupling interaction.[22]

The ^{1}H NMR signals of L do not have unusual splittings, but the shifts provide some useful information about the metal center, the equatorial ligand anisotropy, and the L orientation. ^{1}H NMR shifts for L respond to metal inductive and anisotropic effects and to the equatorial ligand anisotropy.[7,23] The latter effect depends on the average value of ϕ. These effects influence every signal to some extent, but some signals respond primarily to one contribution.

We first consider the Co inductive effect. This effect is best evaluated by examining signals for protons well removed from the anisotropic Co and equatorial ligand.[23] For example, the γ-H signal of py is easily assigned and is further downfield for $[pyCo(N\text{-}CH_2\text{-}CHEL)]PF_6$ (**3**) compared to the I/O and cobaloxime R = CH_3 analogs (Table 7). Thus Co is more electron deficient in **3**. The same conclusion can be drawn from data on the $N\text{-}CH_3$ signals for the *N*-MeImd and Me_3Bzm complexes (Tables 5 and 6).

We next consider the equatorial ligand anisotropy. This effect is best assessed with the proton on the 4-position of the Me_3-Bzm complexes (BH4). This proton passes over the unsaturated parts of the equatorial ligand as the Me_3Bzm rotates, and its position close to the magic angle minimizes the effect of Co anisotropy.[23] The signal is relatively upfield for **1** compared

(21) Günther, H. *NMR Spectroscopy*, 2nd ed.; John Wiley: New York, 1995; p 108.

(22) Calafat, A. M. Unpublished results.

(23) Marzilli, L. G.; Gerli, A.; Calafat, A. M. *Inorg. Chem.* **1992**, *31*, 4617.

Table 8. ^{1}H NMR Shifts (ppm) of [*N*-MeImdCo(*N*-CH_2-CHEL)]ClO_4 in Several NMR Solvents

solvent	H2	H4	H5	C═CH_2	$CoCH_2$	OH···O	imine CH_3	oxime CH_3	NCH_3
acetone-d_6	7.64	6.76	7.32	5.52	3.12		2.35[a]	2.06	3.80
+D_2O				5.82	4.17			2.31	
2.31									
all D-form				5.50	3.13	19.17	2.37[a]	2.07	
(extra signals, H-form)				5.81				2.32	
DMSO-d_6	7.56	6.61	7.39	5.49	3.06	19.02	2.26	2.02	3.74
all H-form				5.78	4.08			2.26	
+D_2O				5.51	3.07				
(extra signals, D-form)				5.79					
$CDCl_3$[b]	7.75	6.64	6.97	5.29	3.01	18.87	2.28	2.05	3.84
all H-form				5.67	3.93			2.36	
+D_2O[b]				5.31		*c*			
(extra signals, D-form)				5.69					

[a] Signal is a doublet. [b] 600 MHz data. [c] Signal still present.

to the (DO)(DOH)pn and cobaloxime R = CH_3 analogs, clearly showing that the equatorial portion of *N*-CH_2-CHEL is anisotropic (Table 5).[7,11,24] This result is expected from the unsaturation of the ligand. Furthermore, since the BH4 shift is upfield of the (DO)(DOH)pn analog, it could be that Me_3Bzm prefers the solid state orientation with BH4 over the olefinic carbons. The *N*-MeImd H4 and py α-H signals for **2** and **3** are further downfield than that for the (DO)(DOH)pn analogs (Tables 6−7).[7,19,23] We believe that the shifts of the signals of these further-in protons reflect less equatorial ligand shielding in **2** and **3** because one double bond has moved further out in the transformation of the (DO)(DOH)pn chelate to the *N*-CH_2-CHEL chelate. However, these signals are influenced by all three factors listed above. Finally, Co anisotropy is difficult to evaluate without a series with the same L and different R's. In this case, R is fixed as the *N*-CH_2 group.

The ^{1}H NMR spectrum ($CDCl_3$) of the product resulting from the treatment of the lariat-type compound [$BrCH_2Co(C_1py)$]-ClO_4 (Chart 1) with methoxide has the characteristic features of the spectra of the other complexes containing a Co−N−C ring: two olefinic doublets, three methyl singlets, and two one-proton singlets (Table 7). The product undoubtedly contains the same metallacyclic ring and the analogous altered macrocycle. The pyridyl signals have shifts characteristic of axial ligation. Thus, the metallacycle formation converts the lariat-type N_5 chelate to a sexadentate chelate with an unusual N_5C type of denticity (Chart 2, [Co(*N*-CH_2-C_1pyCHEL)]$^+$).

The D-Exchanged Form. The ^{1}H NMR spectra of the analytically pure [LCo(*N*-CH_2-CHEL)]X complexes often contained closely spaced signals, including most often the two olefin doublets. These together summed to give the intensity predicted for the signal; the smaller peak was typically about one third the size of the major peak. We have noted previously that the X counterion can displace a weak L in low-dielectric solvents such as $CDCl_3$. Therefore, we used the polar solvents acetone-d_6 and DMSO-d_6 and the strong ligand *N*-MeImd. Extra signals were observed for the *N*-MeImd complex (**2**) (Table 8). The number, resolution, and size of the extra signals were greater in acetone-d_6. Sufficient D_2O (10 μL) was added to an acetone-d_6 solution of **2** for complete D exchange of the O−H···O signal. Under these conditions, we observed only the expected number of signals (Table 8). In contrast, the original acetone-d_6 solution of **2**, containing presumably both residual H_2O and D_2O, had a more complicated spectrum, with two *sets* of olefin doublets, *two* singlets for one of the $Co-CH_2$ protons, two imine CH_3 doublets, and two *pairs* of oxime CH_3 singlets (Table 8). The related signals were of comparable (∼1:1) but unequal intensity. Addition of D_2O to a $CDCl_3$ solution of **2** (Table 8) resulted in an increase in size of the small extra signals, but there was overlap at 300 MHz. However, the 600 MHz spectrum clearly has two separate sets of two doublets in this solvent.

Extra signals for the D-form of a compound with a slightly different N_4C chelate, [*N*-MeImdCo(*N*-CH_2-Me_2pnCHEL)]PF_6 (Chart 2), were observed in acetone-d_6 (Supporting Information). Traditional I/O-type compounds do not exhibit this isotope effect. For the acetone-d_6 spectrum of [*N*-MeImdCo-((DO)(DOH)pn)$CH_2CO_2CH_3$]ClO_4[18] with added D_2O (enough to D-exchange the O−H···O), no additional equatorial CH_3 signals appeared, nor did the signals shift. However, the signal for the $Co-CH_2$ group appeared as two singlets in the original acetone-d_6 spectrum (incomplete exchange of O−H···O).

We do not believe that the isotope effect could arise from the differences in inductive effect of H and D. If this were the case, we would expect a very similar effect on the oxime CH_3 signal of traditional I/O compounds, and this was not found. The shifts of the oxime O−H···O and CH_3 signals for the unaltered half of the equatorial ligand are very similar to those for the I/O compounds. Furthermore, the O- - -O distances are not unusual in the new model system. The I/O compounds have an O- - -O distance of 2.44−2.47 Å,[7,25] cobaloximes have an O- - -O distance of 2.48−2.53 Å,[14,26] and the O- - -O distance of **1** is 2.47 Å. These comparisons suggest that the methyl groups are similar in electronic properties and, therefore, would be subject to an inductive effect if such an effect were responsible for the isotope shift. We suspect that the isotope effect is large enough to be detected in the new compounds because the weaker "H-bonding" ability of D vs H leads to small differences in geometry. Such differences could arise because the N_4C chelate is somewhat strained and the O- - -O distance may increase in the D-form. NMR is a sensitive technique, however, and it is doubtful that such a structural change would be large enough to be detected by X-ray diffraction methods.

High-pH Reactions. The rate of Co−C−N ring formation increased with basicity. However, subsequent reactions at very high pH's made obtaining kinetic data impractical.[1] We have now investigated the principal product of the subsequent reaction at high pH.

Aliquots of a reaction solution of [H_2OCo((DO)(DOH)pn)-CH_2Br]ClO_4 at pH 13 were withdrawn at several different time intervals, neutralized, and evaporated to dryness. *N*-MeImd was added to each residue to facilitate identification of the complexes by ^{1}H NMR spectroscopy (DMSO-d_6). In the spectrum of the residue after 16 min reaction time, the imidazole integrals indicated ∼30% [*N*-MeImdCo((DO)(DOH)pn)CH_2Br]ClO_4, ∼40% [*N*-MeImdCo(*N*-CH_2-CHEL)]ClO_4 (**2**), and ∼30% of a

(24) Polson, S. M.; Cini, R.; Marzilli, L. G. Manuscript in preparation.

(25) Zangrando, E.; Parker, W. O., Jr.; Bresciani-Pahor, N.; Thomas, L. B.; Marzilli, L. G.; Randaccio, L. *Gazz. Chim. Ital.* **1987**, *117*, 307.

(26) Bigotto, A.; Zangrando, E.; Randaccio, L. *J. Chem. Soc., Dalton Trans.* **1976**, 96.

Scheme 1. Possible N_4C to N_4 Chelate Reversion Pathway at pH 13[a]

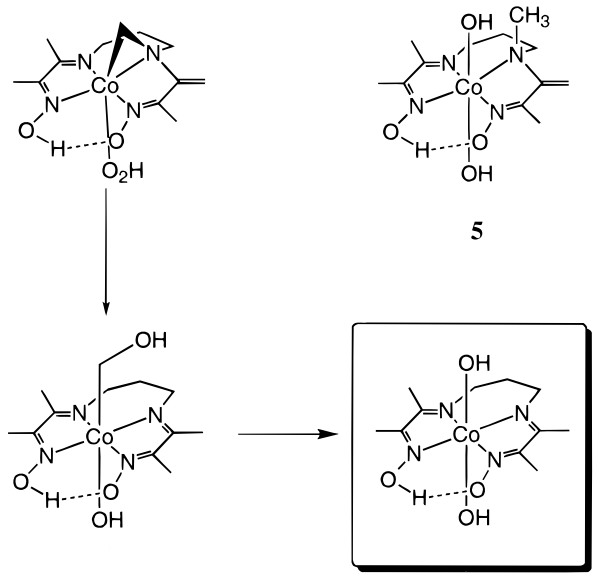

[a] Any pathway involving **5** is unlikely.

new compound, **4**. After 50 min of reaction time, [*N*-MeImdCo((DO)(DOH)pn)CH_2Br]ClO_4 was gone, and the ratio of **2**:**4** was ~1:1. After 100 min of reaction time, the NMR spectrum was relatively unchanged, although the peaks of **4** had broadened significantly.

We then treated [H_2OCo(*N*-CH_2-CHEL)]ClO_4 with base (pH 13) for 50 min. After a workup similar to that described above, the PF_6 salt of **4** was isolated. The ^{1}H NMR spectrum (DMSO-d_6) suggested it was [(*N*-MeImd)$_2$Co((DO)(DOH)pn)]$(PF_6)_2$, an assignment confirmed by adding independently synthesized [(*N*-MeImd)$_2$Co((DO)(DOH)pn)]$(ClO_4)_2$ to the NMR sample. Thus, the N_4C chelate reverts to the traditional N_4 chelate. Before the addition of acid, the reverted complex probably is [Co((DO)(DOH)pn)$(OH)_2$] or [(H_2O)Co((DO)(DO)pn)(OH)].

Several mechanistic pathways can be envisioned for the reversion, which requires that at least two events, Co−C bond cleavage and C−N bond cleavage, occur. If the cleavage events occurred simultaneously, the reaction would be tantamount to the extrusion of a reactive carbene. Carbenes are normally generated under harsh conditions or with very reactive precursors.[27] Carbene generation by a strong (usually organometallic) base involves methylene precursors with very good leaving groups.[27] In the present case, a C−N bond of **2** would need to be cleaved. Such a bond is not readily cleaved without the presence of catalysts.[28] Furthermore, we found that [LCo(*N*-CH_2-CHEL)]ClO_4 complexes contain stronger Co−C bonds than those of other B_{12} models.[1] Therefore, the simultaneous cleavage of both Co−C and Co−N bonds is unlikely. If Co−C bond cleavage of **2** occurred first (to give **5**, Scheme 1), the initial ring-opened intermediate would have to undergo unfavorable C−N cleavage. Finally, C−N cleavage is a more favorable reaction when the bond is contained in a three-membered ring (an aziridine).[29,30] If Co−N bond cleavage occurred first, a CH_2OH I/O intermediate would form after addition of a proton to the initially olefinic C (to create an imine methyl group). This intermediate would then undergo facile Co−C bond cleavage to give a non-alkyl I/O complex (Scheme 1). Although there is no example of such Co−C cleavage of a CH_2OH complex, we favor this pathway because such CH_2OH adducts cannot be synthesized presumably because they are unstable[31,32] and because base-catalyzed Co−C bond cleavage is known for LCo(DH)$_2$R at pH 13 (Chart 1).[33] Co−C bond cleavage only after the ring opening is consistent with our observations suggesting that [LCo(*N*-CH_2-CHEL)]ClO_4 complexes contain stronger Co−C bonds than those of other B_{12} models.[1]

Conclusions

Our study of [LCo(*N*-CH_2-CHEL)]$^+$ models showed clear differences in steric bulk between *N*-MeImd and Me_3Bzm. We found that the sum of the four *cis* N−Co−N(5) bond angles is a useful measure of both L bulk and equatorial ligand distortion. Despite the greater upward bending of the *N*-CH_2-CHEL chelate, the Co−N(5)−C bond angles were similar to angles found previously in models with more planar equatorial ligands and in cobalamins.[7,34−36] This result suggests that these angles are determined primarily by the direction of the Me_3Bzm lone pair and not by steric clashes with the equatorial ligand. Nevertheless, specific *cis* N−Co−N(5) bond angles do suggest that Me_3Bzm bulk is greater than *N*-MeImd bulk. Me_3Bzm does not fit well into the pocket created by the metallacycle, and solution data suggest that the Me_3Bzm ligand lies over the olefinic double bond, as in the solid state. Because of the complexity of the NMR data, the solution analysis must be labeled as tentative. However, the NMR data clearly show that the lariat analog, [Co(*N*-CH_2-C_1pyCHEL)]$^+$, contains a novel N_5C chelate with the pyridyl N coordinated *trans* to the axial CH_2.

^{1}H NMR shifts of some signals of the protio (O−H···O) and the deuterio (O−D···O) [LCo(*N*-CH_2-CHEL)]$^+$ forms are clearly different. This D-isotope effect on shifts, not observed in normal I/O complexes, is an unusual phenomenon. It may arise from the strained nature of the quinquedentate ligand; the weaker "H-bonding" of the deuterio form leads to differences in Co−N bond distances, which in turn result in the larger than normal isotope effects observed.

The presence of strain in the metallacycle is also consistent with its reactivity to base observed at pH 13. The product lacks the axial CH_2 moiety and has a normal I/O chelate. The most likely mechanism for this N_4C to N_4 chelate reversion is a stepwise process consisting of the following steps: cleavage of the C−N bond, formation of Co−CH_2OH and imine methyl groups, and cleavage of the Co−CH_2OH bond.

Acknowledgment. This work was supported by NIH Grant GM 29225 (to L.G.M.). Instrument purchases were funded by the NIH and the NSF. NSF Grant ASC-9527186 supported our use of the Internet for remote collaborative research. We thank Dr. Antonia Calafat for communicating the 2-D NMR assignments and Dr. Renzo Cini for useful discussions.

Supporting Information Available: Packing diagrams and listings of crystallographic data, atomic coordinates, displacement parameters, and bond distances and angles for compounds **1** and **2**, as well as tables of elemental analyses and additional NMR data (15 pages). Ordering information is given on any current masthead page.

IC970022V

(27) Carey, F. A.; Sundberg, R. J. *Advanced Organic Chemistry, Part B: Reactions and Synthesis*, 3rd ed.; Plenum Press: New York, 1990; p 516.
(28) Murahashi, S.; Yano, T. *J. Chem. Soc., Chem. Commun.* **1979**, 270.
(29) Paquette, L. A. *Principles of Modern Heterocyclic Chemistry*; W. A. Benjamin, Inc.: New York, 1968; p 25.
(30) Newkome, G. R.; Paudler, W. W. *Contemporary Heterocyclic Chemistry*; John Wiley & Sons: New York, 1982; p 350.
(31) Brown, K. L. Personal communication.
(32) Elroi, H.; Meyerstein, D. *J. Am. Chem. Soc.* **1978**, *100*, 5540.
(33) Brown, K. L. *J. Am. Chem. Soc.* **1979**, *101*, 6600.
(34) Rossi, M.; Glusker, J. P.; Randaccio, L.; Summers, M. F.; Toscano, P. J.; Marzilli, L. G. *J. Am. Chem. Soc.* **1985**, *107*, 1729.
(35) Kratky, C.; Färber, G.; Gruber, L.; Wilson, K.; Dauter, Z.; Nolting, H.; Konrat, R.; Kräutler, B. *J. Am. Chem. Soc.* **1995**, *117*, 4654.
(36) Kratky, C. In *Proceedings of the 4th Symposium on Vitamin B_{12} and B_{12}-Proteins*, Innsbruck, Austria, Sept 2−6,1996; p L6.